



Research Article

# Sonofusion's Transient Condensate Clusters

Roger S. Stringham\*

4124 Kapuna Rd. Kilauea, HI 96754, USA

---

## Abstract

D<sub>2</sub>O cavitation produces Z-pinch jets implanting a target lattice. Measurements, data interpretations, and FE SEM photos explain products heat and <sup>4</sup>He produced in target foils. The picosecond dynamics of a deuteron electron plasma charge separation and pressure pulse produce alpha particles and heat.

© 2014 ISCMNS. All rights reserved. ISSN 2227-3123

*Keywords:* Cavitation, Condensate, Deuteron, Image

---

## 1. Introduction

Over twenty years of work including thousands of experiments have contributed to the explanation of the puzzling and disjointed aspects of sonofusion technology. Using new analytical techniques and data interpretations gives a fresh look at sonofusion processes at a megahertz frequency. Among the resolved problems was the target foil destruction associated with kilohertz low frequency problems. As time passed it appeared that BECs in the form of nuclear condensates would lead to paths that resolved some major problems [1–3]. The excess heat ( $Q_x$ ) was not accompanied by any long-range radiation products. The high densities required to produce the products of alpha particles and heat in sonofusion are similar to the densities of muon fusion. Conditions found in astrophysical steady state systems can be drawn from to help explain what is a very transient terrestrial environment. It might be expected to exist in a picosecond timeframe culminating in a single alpha particle event per implanted cluster. During some sonoluminescence (SL) measurements a new technique was developed for counting photons in the MPPC energy range by the manipulation of the device's saturation mode.

## 2. Review

Sonofusion in the megahertz range uses a 20 mm disk piezo driving the D<sub>2</sub>O cavitation bubble process. The red acoustic wave amplitude,  $Q_a$ ,  $P^+$  to  $P^-$ , finds a resonant bubble, blue  $R_i$  bubble, Fig. 1. Within this  $\mu$ s cycle, the bubble grows to  $R_o$ , then violently collapses to  $R_f$ , dark blue. The emitted photon pulse, SL, shown in green, originates from many  $R_f$

---

\*E-mail: firstgate@earthlink.net

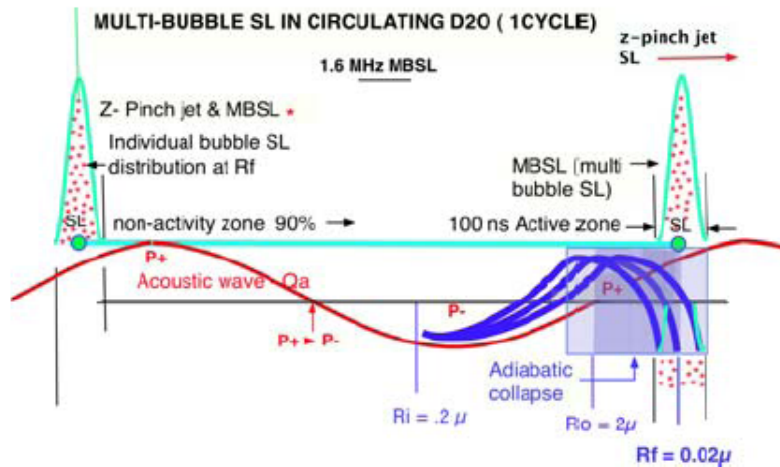


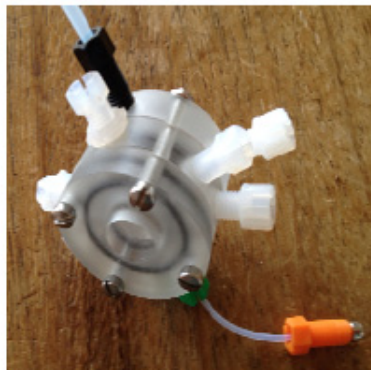
**Figure 1.** The megahertz  $D_2O$  cavitation bubble cycle and violent adiabatic collapse, blue, noted by a 100-fold change in radius, produces Z-pinch jets with SL plasma, green. Z-pinch jets implant the target foil producing DD fusion.

bubbles ( $10^3$ – $10^5$ ), red stars [4–9]. To maximize the SL's photon count and the high-density Z-pinch  $D^+$  jet intensity, one adjusts the acoustic power input,  $Q_a$ . During a 1.6 MHz cycle in the 100 ns active zone, the SL emission pulse and the Z-pinch implantation jets are distributed into a target foil. Over 90% of the cycle is without of any activity. The SL emission shows a 100 ns time period of implant activity when transient charge separated deuteron clusters are produced. An expanded view using the larger knowledge base of low frequency resonant bubbles, 20–46 kHz, in  $H_2O$  and  $D_2O$  studies is extended to the higher megahertz frequency of the  $D_2O$  bubble systems [4,5].

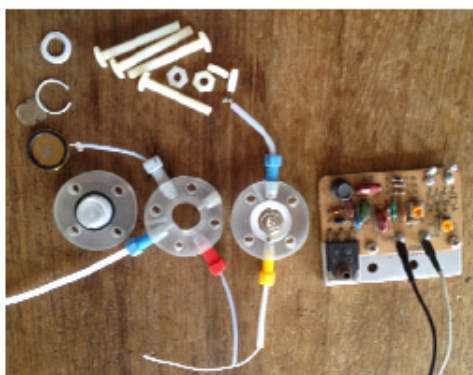
These systems require control over the parameters of temperatures, pressure, and acoustic input. The general piezo bubble mechanics holds for all frequencies studied. The same bubble mechanics should hold for frequencies up to 20 MHz. These higher frequencies systems have the following advantages: they are easier to study; more economical; they produce less damage to target foils; and they produce the same energy density in smaller and more numerous bubbles. Coincidental to the SL emission is the Rf bubble formation of a Z-pinch jet that is located close to the surface of the target foil lattice. The jet is a partial plasma that is squeezed by sheath electrons accelerating and squeezing the jet's contents to higher densities before implanting into the lattice. The jet formation from bubbles is well known, and damage to water handling mechanical devices like pumps and propellers is common.

### 3. Experimental

The megahertz cavitation experiments were carried out in a black felt lined light-proof box 0.4 m on a side, with a fan circulating air through the totally dark experimental system so that the SL could be monitored. SL was a tool, a method of photon monitoring of the plasma character of the collapsed cavitation bubble's target implanting Z-pinch jet. The three parameters controlling SL and cavitation were; the temperature of the  $D_2O$  in the reactor, the argon pressure over the circulating  $D_2O$ , and the acoustic power,  $Q_a$ . It was important to keep the acoustic megahertz piezo polycarbonate reactor cool at its resonance. This is accomplished with the circulation of  $D_2O$ . Small changes in the temperature were accommodated using a feedback type acoustic oscillator that sensed and adjusted to changes in the natural resonating frequency of the reactor. Input power ( $Q_i$ ) was measured by a 0–100 W wattmeter from Ohio Semiconductor, where  $Q_a = 0.3 Q_i$ . The  $20 \text{ cm}^3$  of circulating  $D_2O$  via a 6 mm FMI displacement pump operated at a flow rate of 1.02 g  $D_2O/s$ .



2(a)



2(b)

**Figure 2.** (a) The 1.6 MHz reactor. (b) The disassembled reactor and  $Q_a$  oscillator, Pd target foil is third object from bottom, left corner. It was clamped together with Nylon or stainless steel bolts.

The tubing was 1.5 mm stainless steel and fluorinated ethylene polymer. They were used as reactor connections for  $D_2O$ , argon gas, electrical acoustic ports, and 0.07 mm diameter K-type thermocouples (TCs). These connections were completed at the polycarbonate reactor, with 6 mm tapped Omnifit fittings, Fig. 2(a). Temperature data was collected every second. In the pump's  $D_2O$  circulation path was a 1.5 m  $\times$  1.5 mm stainless steel coil tube heat exchanger in 2 L of water and a sintered stainless steel 10  $\mu$ m filter that removed particulates. Next in the flow path was the TC used to measure  $D_2O_{in}$  at the reactor inlet. The cavitation residence time of  $D_2O$  in the reactor was about 1 s. The TC measurement at the reactor outlet monitored  $D_2O_{out}$ . The other TC was located at the bottom as the  $D_2O_{in}$  flow entered, completing the  $\Delta T$  measurement. As the flow continued it passed through a visual flow meter, from K/E, with a 100 cm<sup>3</sup>/min maximum. From there the  $D_2O$  passed to a 50 cm<sup>3</sup> stainless steel and Pyrex bubbler that was connected to a vacuum line that managed the fluids and gases. In the bubbler was 20 cm<sup>3</sup> of argon saturated  $D_2O$  that circulated to the pump, completing the  $D_2O$  cycle. Figure 2(a) shows the disassembled 1.6 MHz reactor and the acoustic oscillator.

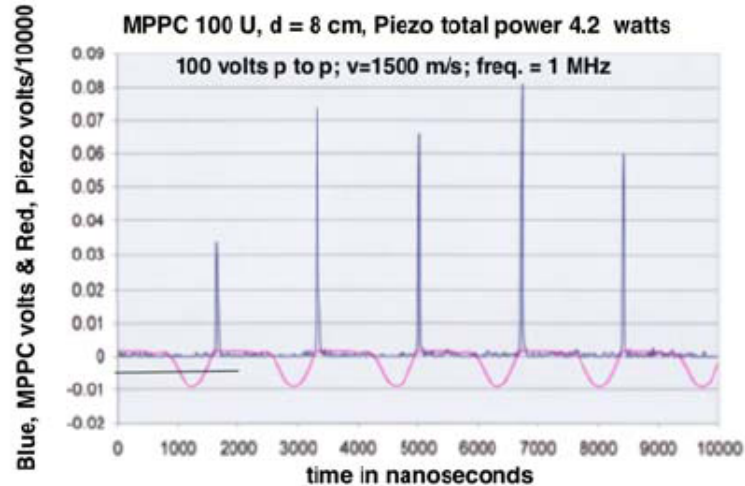


**Figure 3.** Measurements of SL MPPC differences between blocked and unblocked photons were made, blue trace. The MPPC was located 8 cm from the megahertz reactor. The red trace is a 100 V MHz acoustic wave the  $Q_a$  input, note the coupling of SL to  $Q_a$ . The SL trace in Fig. 1 green trace of 100 ns SL photons. Only in 100 ns was there any activity.

### 3.1. SL and photon counting

The acoustic input ( $Q_a$ ) of 1–16 W powered the piezo at a megahertz frequency and was monitored by channel 1 of the oscilloscope. The photon counter, Multi Pixel Photon Counter, MPPC S510362-11 series from Hamamatsu, with a millivolt output was monitored by channel 2. The DC volt input to the MPPC was from a HP 6634A power supply. The MPPC device had a photon counting area of 1 mm<sup>2</sup> that was placed 8 or 16 cm from the reactor window. The MPPC outputs were frequency and pressure coupled shown in Fig. 3 in blue and red. It took many runs to establish the separation of MPPC dark current from the SL photon emission.

There was no radio frequency (RF) interference in the difference measurements (MPPC open-beam SL minus blocked-beam SL) of the SL photon count. The D<sub>2</sub>O photon intensity was 10<sup>9</sup> per cycle and more diffuse than single bubble SL. It has an order lower intensity than H<sub>2</sub>O, and was not visible to the naked eye [9].

### 3.2. Piezos, Z-pinch jets

The favored 1.6 MHz piezos, run at 50 W from the wall,  $Q_i$ , rather than the 20 kHz at 600 W  $Q_i$ , and they produce in 10<sup>4</sup> smaller volume 100 times more bubbles, which have the same energy density of the low frequency systems. The bubbles collapse adiabatically producing the dissociated plasma of D<sub>2</sub>O. At the collapse at Rf, SL and a Z-pinch jet are produced, Fig. 1. The velocity of the Z-pinch jet's sheath electrons generates a magnetic compression, a Z-pinch. The magnetically compressed Z-pinch jet transmits the dense plasma, implanting deuterons and free electrons into the target lattice forming the concentric condensates that will be shown later. Coincident with the Z-pinch jets is the SL monitored with a MPPC and suggests the condition of the plasma via SL photon intensity.

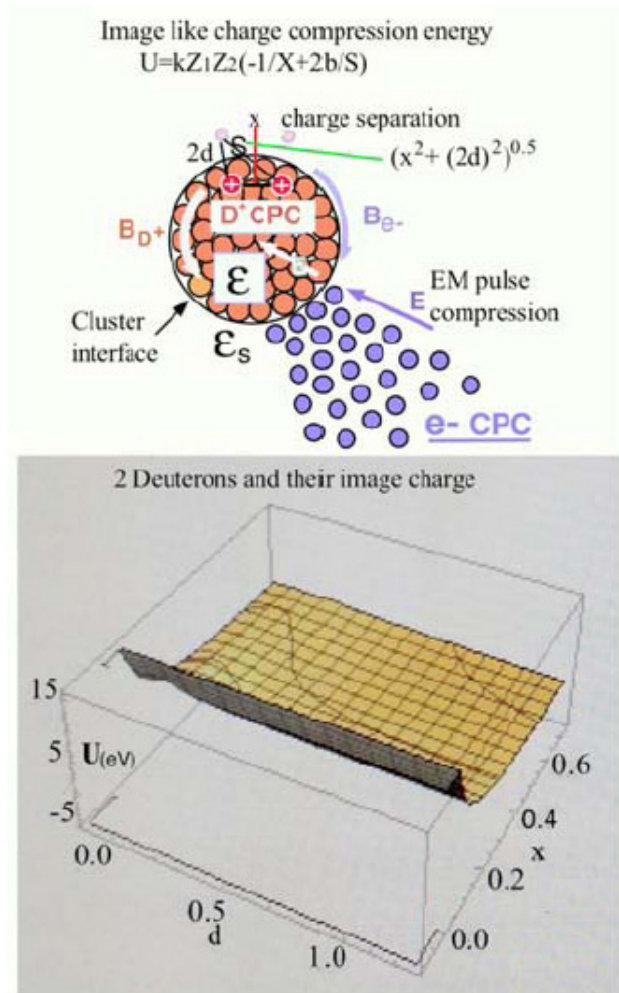


**Figure 4.** Top is the cluster implosion image and EM pulse energy of the 2 concentric charged particle condensates that form the 2 concentric condensates of D+ and 2e<sup>-</sup>. Blue balls represent Cooper Pairs and orange balls, deuterons. The cluster’s unit image is formed of the 2 D+ red balls, and across the interface are the 2 D+ violet image balls of the electron condensate. The d, in Å, is the interface distance to the D+ image charge, pink ball, and to the D+, red ball. The image-charge particle separation x, in Å, between 2 deuterons, red balls, is squeezed during the concentric condensate implosion [1]. Altogether they form the geometry of the image charge attractive energy of deuteron separation. Bottom shows the beginning implosion of particle closing separation energy U<sub>(eV)</sub>. The fusion squeeze is a picosecond event. Apply the image units to n= 10<sup>2</sup> pairs that make up the total spherical interface system. Blue and white arrows show the EM E field compression. The EM B fields, white and blue arrows, tend to cancel.

### 3.3. Cluster EM compression pulse

The EM driven implosion of the sub-nanometer deuteron cluster is represented as a spherical cluster of high density orange balls, Fig. 4, with a surface interface area of  $4\pi r^2$  squeezed by an equally high density of free electrons. The

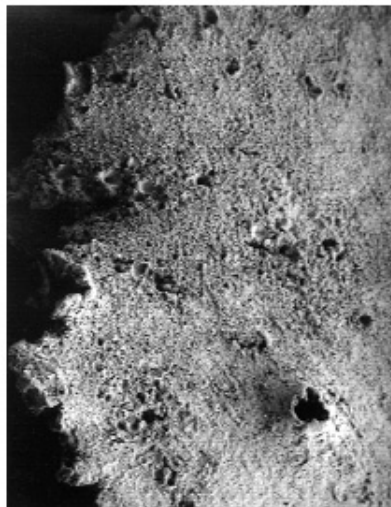


Fig. 5(a)



Fig. 5(b)

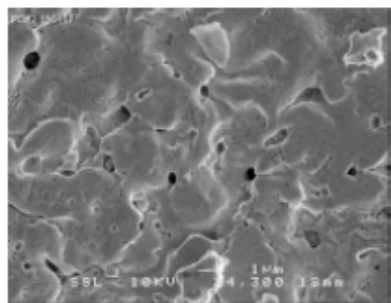


Fig. 5(c)

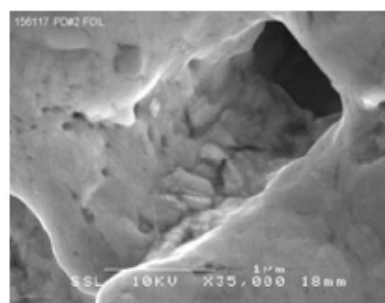
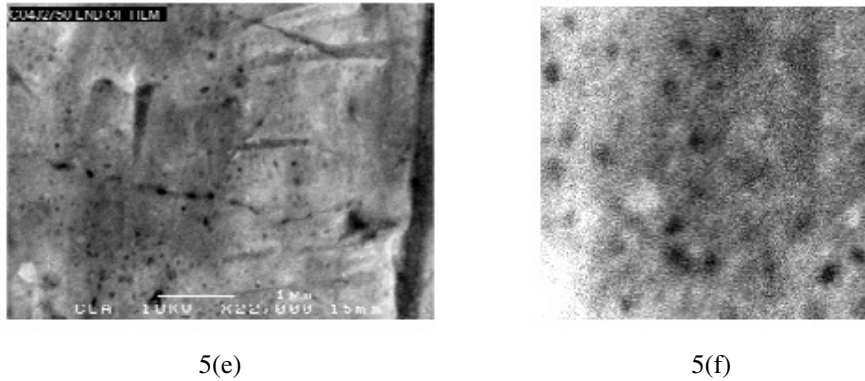


Fig. 5(d)

electrons, violet balls, spherically surround the deuteron cluster, and at these extreme densities will likely be coupled as Cooper Pairs, bosons [2]. These densities will form a free electron condensate phase that squeezes the interface surface with coulombic plasma pressure power. For a time period of less than a picosecond these particles move towards their common center. The EM pressure power pulse increases to values in spherical symmetry equivalent to those spatial separations in the muon molecular ion. The density is high enough to allow for one destructive fusion event, and this is what is measured in ejecta sites. See FE SEM photos of Fig. 5(e). The high density picosecond electron electromagnetic pressure power pulse, EM, at the cluster interface  $k\Sigma q_1 Q_2 / r^4 \text{sec}_1$  is the squeezing pressure power, where  $q_1$  is 1 electron,  $Q_2$  is D+ cluster,  $r$  is the interface radius, and  $k$  the constant for SI units. Opposing this squeezing pressure power is the Coloumb repulsion pressure power at the interface  $k\Sigma q_3 (Q_2 - q_3) / r^4 \text{sec}_2$ , where  $q_3$  is a D+. The ratio is  $\text{sec}_2 / \text{sec}_1$  equals  $10^{12}$  more pressure power at the interface during the interface compression.

There is no chemical activity at the interface as it is too hot and fast for the deuterium atom formation. The deuterons and free electrons have the same compressing acceleration at the interface. The magnetic fields and forces are tangent to the interface and surround the cluster's compression space. These magnetic fields cancel at the interface, with equal



**Figure 5.** (a) SEM photo of a Pd target foil with multi-size ejecta sites; frequency of 20 kHz; scale 0.5 mm = 10  $\mu$ . (b) SEM photo of an ejecta site detail of 5a; scale 1 mm = 1  $\mu$ . Photos by John Dash. SEM photo of a Pd target foil with multi-size ejecta sites; frequency of 46 kHz; scale 1 mm = 1  $\mu$ . (c) SEM photo of a Pd target foil with multi-size ejecta sites; frequency of 46 kHz; scale 1 mm = 1  $\mu$ . Detail from 5c SEM photo; scale 1 cm = 1  $\mu$ . Photos by Jane Wheeler. (d) Detail from 5c SEM photo; scale 1 cm = 1  $\mu$ . Photos by Jane Wheeler. (e) SEM photo of a Pd target foil with a single size ejection site; 1600 kHz sites; scale 0.5cm = 1  $\mu$ . (f) A 1 square  $\mu$ m detail from 5e SEM photo showing ejecta sites of single DD fusion events  $\diamond$  about 20 MeV; scale, one ejecta site = about 50 nm in diameter. Jane Wheeler.

compression collapse velocities. The E fields, green and blue, from the imploding deuterons and electrons are additive. The picosecond EM pulse at the interface is compressed by an increasing like-charge cluster compressing pressure at the interface, but is eventually overcome by the increasing repulsive pressure. The EM pulse reaches the critical fusion density before the pressure pulse collapse. The adiabatic compression heating of the cluster is reduced by the loss of surface deuterons, evaporative cooling. This adds to the momentum of the cluster's implosion. This cooling gives the deuteron condensate more stability during compression. As the pulse compresses the cluster, a fusion environment is reached; fusion occurs and the cluster's particles revert back to D<sub>2</sub>O. The ejecta carry the  $Q_x$  and  ${}^4\text{He}$  into the D<sub>2</sub>O circulation. For a cluster originating from  $n_{\text{D}_2\text{O}}$  equaling 10,000 D+ the recombination energy is 0.007 that of a single 24 MeV fusion event. Note this when looking at ejecta sites (Fig. 5(f)).

### 3.4. Image charge of two deuterons and CP

At the accelerating interface both D<sup>+</sup> and e<sup>-</sup> accelerate together to the center of the cluster. Residual concentric spherical magnetic fields with the same center are sandwiched at the interface between two condensates in compression [1,2], with a large difference in their respective permittivity,  $\epsilon$ . The image-charge system provides an alternate mechanism to the EM pressure power pulse for reducing deuteron separations. Under the conditions of high density, charged particles across an interface of a large  $\epsilon$ g differences, these like-charge particles become attractive. The imploding imploding clusters consist of two concentric BECs Cooper Pairs (CP) and deuterons. These two particle groups have relative permittivities proportional to their mobility across their mutual surface interface, Fig. 4. top. The electron cluster has a relative permittivity of  $\epsilon_s$ . The imploding accelerating interface of the deuteron BEC has a permittivity  $\epsilon$ . At the interface, between the two condensates, the  $\epsilon_s/\epsilon$  ratio of the relative permittivities is  $10^3$  based on their relative mobilities. The image charge system's permittivity factor  $b = (\epsilon - \epsilon_s)/(\epsilon + \epsilon_s) = -1$  ( see Lawandy's description [1]). The effective squeeze range for  $b$  is from  $-0.5$  to  $-1.0$ , with  $-1$  giving the maximum effect. This sonofusion system's  $b$  is close to  $-1.0$ , and provides an excellent environment for the deuteron's attractive image charge energies to reduce deuteron separation  $x$  as  $d$  diminishes below  $\text{\AA}$  levels. The cluster's particles are arranged as onion-skin d layers, from the interface to the center (five layers of deuterons,  $n = 10^2$ ). A collective application of  $n = 10^2$  of paired



like-charges produces  $U(x)$  in eV. When  $b = -1$ , it shows the mechanics of reduced separation  $x$  of like-charge image energies in the deuteron cluster in the sub-picosecond range.  $U(x)$  is 15 eV and increasing. A picosecond duration at these densities is a satisfactory period for DD fusion to occur. The number of fusion events is measured by the survey count of ejecta sites shown in SEM photos in Fig. 5(f).

### 3.5. The nuclear and electron condensate environment

These condensates in this case are different, and not like the more often discussed condensate of cold Boson atoms. The cluster is a self-focusing layered spherical collection of Bosons, deuterons and CP, Fig. 4. For a picosecond there are no associated electrons inside the interface of the cluster during the EM pressure power pulse. The cluster is expected to have the properties of a deuteron nuclear Boson condensate cluster. The cluster is squeezed by the exterior CP condensate, as the separation between fm sized charged deuteron particles is decreasing. The two concentric condensates have very high critical temperatures,  $T_c$ , across their interface [3].

The uniqueness of the D+ condensate character is outlined here. The deuterium atom, after removal of its one  $e^-$ , is a single charged boson nucleus and is unique in the family of particles at 2.14 fm. Its nucleus is the most easily dissociated. The deuteron has only one measured energy level, its ground state,  $E_0$ . The deuteron has a large  $E_1 - E_0$  energy level separation greater than its dissociation of 2.23 MeV and supports a high  $T_c$  of millions of degrees. A picosecond environment of compressing condensates produces DD fusion events with no measurable radiation products. The energy levels are nuclear, not chemical. Experiments show that sonofusion's  $Q_x$  cluster dynamics is the sum of the DD fusion events at a rate of  $10^{13}$  per second that is also the sum of the frozen target cluster ejecta site count, Fig. 5(e). The two deuterons and CP, are separated and compressed at the cluster's spherical interface. The residual of opposite and tangent magnetic fields generated by the separated charge movement to their common center, Fig. 4, are excluded from the condensates. The canceling magnetic fields at the interface are compatible with the condensate's Meissner exclusion. The BEC compression heating from within the deuteron cluster looks for relief through a cooling mechanism presented as the evaporation of deuterons from the cluster interface [9]. This flow of mass also provides momentum compression, and may progress to the point of less than 100 remaining deuterons in the deuteron cluster for the single DD fusion event per cluster at a megahertz frequency.

### 3.6. The DD fusion in the cluster

The deuteron cluster's compression movement during a picosecond approaches  $10^{-12}$  m or closer, a separation that is similar to that of muon fusion [1,2]. The DD fusion has the time and the density (separation) for a product path to  ${}^4\text{He}$  and  $Q_x$ . The immediate rate-energy transfer in the deuteron CP condensate as the  $Q_x$ , the heat of fusion in a disrupted cluster, quenches the potential for a 24 MeV gamma. The mechanism is too slow (in the range of one gamma photon oscillation,  $10^{-22}$  s). The target foil's SEM photos show, at these megahertz frequencies, that the DD fusions are single events and leave ejecta sites as their footprint [4,8]. The measurement of target foil severity of damage is related to the piezo acoustic driven frequency. The information gathered from SEM photos of target foil damage at the low frequency of 20 and 46 kHz shows extensive foil damage from multiple fusion events. Some larger  $10\ \mu\text{m}$  ejecta sites from the low frequency piezos show many sub-micron spheres of recondensed vaporous target foil in the ejecta cavity, and few single fusion events. The megahertz exposed foils in Fig. 5 show a trend to much less target foil damage and many more eject sites, all of the same energy. The energy on the megahertz exposed foils showed these sites, Fig. 5(f), are  $20 \pm 10$  MeV ejecta sites, with a single event of one alpha particle per cluster [9].



### 3.7. Acoustic frequency effect

The measurement of target foil damage severity is related to the piezo acoustic driven frequency. The lower the frequency the more severe the target foil damage. The information gathered from SEM photos of target foil

### 3.8. Cluster's ejecta site at low frequency

The cluster's single DD fusion event is generated during the picosecond after the Z-pinch plasma implantation of deuterons and electrons. Fusion products and debris are ejected into circulating D<sub>2</sub>O. The ejecta site size and depth are shown in the SEM photos, Fig. 5 [4]. A survey of the size distribution of ejecta sites in the Pd target foil exposed to 46 kHz of cavitating D<sub>2</sub>O are shown in Fig. 6. The single events are few, and quite different than the megahertz system, and are surveyed in the 1 μm square at three times the resolution, lower left in Fig. 6. The larger SEM field of ejecta site damage represents thousands of DD fusion events.

### 3.9. Data, heat (calorimetry) and <sup>4</sup>He

The 1.6 MHz reactor flow-through calorimetry using K-type thermocouples measured  $T_{\text{out}} - T_{\text{in}}$ ,  $\Delta T$ , of the circulating D<sub>2</sub>O. And an in-line flow-meter measured the D<sub>2</sub>O mass-flow/second. The low mass of the reactor at half the mass of the D<sub>2</sub>O flow per minute is an advantage. The  $\Delta T_x$  (D<sub>2</sub>O flow in g/s)  $\times$  4.184 = watts out ( $Q_o$ ).  $Q_a$  is the measured acoustic power input.  $Q_o - Q_a = Q_x$  and is the heat of fusion for the reaction  $2D^+ = \alpha + 23.8$  MeV and equals  $mc^2$  (the mass deficit as heat not a gamma ray). The graph  $Q_a$  versus  $Q_x$  indicates close to a linear relationship shown in Fig. 4. DOE mass spectral analyses of sampled gases circulating with the D<sub>2</sub>O from a 20 kHz reactor after a 19 h run established the presence of <sup>4</sup>He in an amount of  $552 \pm 2$  ppm in their report [4,6].

## 4. Discussion

It is remarkable that sub-nanometer transient clusters will fuse when compressed as in Inertial Confined Fusion to produce fusion heat,  $Q_x$ , and <sup>4</sup>He with no measureable neutrons or gammas. Sonofusion does that, and depends on

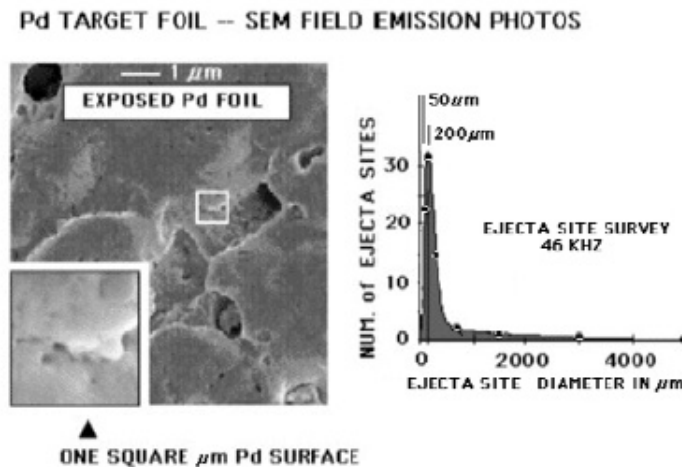


**Figure 6.** SEM survey of an exposed 46 MHz Pd target foil and the distribution of ejecta sites produced by DD fusion in cluster ejecta sites.

a picosecond spherical subatomic size cluster,  $10^{-11}$  m, in a deuteron condensate cluster implosion where densities equivalent to those of muon fusion produce  $Q_x$  and  ${}^4\text{He}$ . Sonofusion energy production is focused just below the target foil lattice surface in clusters that produce ejecta sites. Experimental results can be expanded to explain other low temperature fusion technologies. The megahertz cavitation of argon gas saturated  $\text{D}_2\text{O}$  produces transient spherical condensate deuteron clusters that drive the cluster's interface like a spherical piston into the DD fusion mode. Condensates of deuterons and CP and their subtractive tangent magnetic fields, and their respective perpendicular additive electric fields form a spherically centered dipole pulse, Fig. 4. Both CP and deuterons, on either side of their common interface, accelerate to the cluster's center during the picosecond compression pulse. In these extreme high-density cluster compression environments of CP, two electrons will be favored over one. Some deuterons will ultimately fuse, destroying the cluster, and are identified by their FE SEM ejecta site photos and calculated energies, Fig. 5(e). The rest of the clusters will revert back to  $\text{D}_2\text{O}$ , a path thousands of times less energetic than the  $Q_x$  of a single fusion event. The cluster survey count extrapolates to  $10^{13}/\text{s}$  of the 50 nm diameter ejecta sites per second (a survey estimate and also the calorimetry heat measurements) in a 1.6 MHz exposed target foil. The exposure indicates that less than 10% of a  $1\text{ cm}^2$  Pd-target foil is used and less than 10% of the time is actively involved. Each acoustic megahertz cycle destroys old sites as new sites are produced in the next cycle. Each ejecta site originates from a single 23.8 MeV fusion event, see Fig. 5(f). The number of ejecta sites is equivalent to the number of fusion events per second. The ejecta site count calculation is 38 W of  $Q_x$ , The measured calorimetric calculation is  $57\text{ W} \pm 10\%$  for a  $15.2\text{ W } Q_a$  input, shown in Fig. 7. The deuteron cluster's evaporative cooling, where interface surface deuterons are ejected through a mass of free electrons that are too hot to recombine until cool-off that is well beyond the interface.  $\text{D}_2\text{O}$  is the choice of cavitating liquids because of its recombination characteristics after the heat pulse. The deuteron spherical size is  $2^+$  fm and expands at recombination to an atom size of  $2^+ \text{ \AA}$ . Adding an electron to  $\text{D}^+$  effectively removes heat from the cluster and adds compression and momentum from the surrounding exterior of the Pd lattice [9].

Nabil Lawandy [1] explains into cluster squeezing pressures via the accelerating CP– $\text{D}^+$  interface. The image-charge separation reduction of like-charge particles is the mechanism that produces fusion events. Compressive pressures result from large permittivity differences between free  $e^-$  as CP and  $\text{D}^+$  cluster condensates across the interface depend on their relative mobility. Image-charge energies reduce deuteron separations that parallel other transient EM pressure pulses that coulombically squeeze the cluster's DD fusion probability into reality. The cluster's transient lifetime of a picosecond, with its small squeezed deuteron clusters, have densities close to  $10^{36}\text{D}^+/\text{m}^3$ . The squeeze produces one

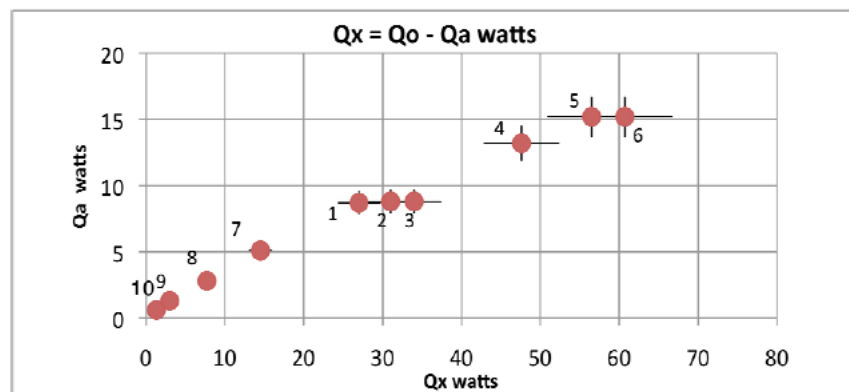


Figure 7. The megahertz  $Q_x$  flow-through calorimetry is shown in the time sequence of the acquired 10 data points [7].

fusion event per cluster in megahertz driven D<sub>2</sub>O cavitation. The deficit energy,  $Q_x$ , will be dispersed from a nuclear D<sup>+</sup> condensate as heat. A superconducting environment rejects any radiation mechanism.

The  $T_c$  measurements were made at intervals at the beginning of the off mode as the reactor piezo drive was programmed with a duty cycle of 120 s on and 120 s off.  $T_c$  measurements were made every second and were back calculated to the time of the start of the off mode to determine the  $\Delta T$  and  $Q_o$ . This eliminated any possible radio frequency interference from the megahertz piezo during  $T_c$  measurements. The low mass reactor was close to steady state temperature after one minute of piezo running time. The total power in,  $Q_i$  was measured by 0–100 W power meter from an Ohio Semiconductor,  $Q_a = 0.3Q_i$ , where  $Q_i$  was the measured total input power. The data was taken at different  $Q_a$  measuring the SL intensity and the watts out,  $Q_o$ , where  $Q_x = Q_o - Q_a$  (see Fig. 7). The length of each series of runs was about 20 min at a measured acoustic power input,  $Q_a$ .

These small 20–50 g single unit megahertz sonofusion reactors, with a  $2 \times 20$  mm piezo disk, can be ganged together to make any sized device. <sup>4</sup>He in target foils will be stable for years, and can be analyzed for <sup>4</sup>He content and stable isotope changes at any time. Sonofusion's energy future can be viewed as a high impact energy technology that may eventually replace the need for hydrocarbon based energy providers. D converts to non-polluting <sup>4</sup>He and radiation free heat,  $Q_x$ . No long-range radiation products have been measured during experiments on a variety of target foils. The total calculated sonofusion energy, excluding  $Q_x$ , should not exceed the  $Q_a$  input. At 100 deuterons the value is 0.2 W, when  $Q_a$  is 15 W producing  $10^{13}$  fusion events per second. Smaller clusters and higher megahertz frequencies show a promising future for sonofusion. This is a changing model for sonofusion.

## Acknowledgements

Support of this work is in the form of moral support from my family and friends.

## References

- [1] N.M. Lawandy, Interaction of charged particles on surfaces, *Appl. Phys. Lett.* **95** (2009) 234101-1-3.
- [2] H Abuki, T. Hatsuda and K. Itakura, Color superconductivity in dense QCD and structure of Cooper Pairs, NSF-ITP-02-45 hep-ph/0206043, 4 June 2002.
- [3] Masahito Ueda, *Fundamentals and New Frontiers of BEC* ( World Scientific, Singapore, 2010 ). ISBN-10 981-283-959-3.
- [4] R. Stringham, Sonofusion, deuterons to He experiments, *ACS source book #2*, 2009, pp. 160–167.
- [5] R. Stringham, When bubble fusion becomes sonofusion, *J. Cond. Nucl. Sci.* **8** (2012) 1–12.
- [6] R.S. Stringham, Ti produces tritium that decays to helium 3, *CMNS, Proceedings 15*, Rome Italy, V. Violante and F. Sarto (Eds.), 5–9 Oct. 2009.
- [7] R.S. Stringham, Low Mass 1.6 MHz sonofusion reactor, *Proc. ICCF-9*, Marseille, France, J.P. Biberian (Ed.), 31 Oct.–5 Nov. 2004.
- [8] R.S. Stringham, Cavitation and fusion, *Proc. ICCF 10*, Boston, USA, P.L.Hagelstein and S.R. Chubb (Eds.), 24–29 Aug. 2003.
- [9] R.S. Stringham, Model for electromagnetic pulsed BEC experiments, *JCMNS, Proceedings ICCF 16*, Chennai, India, M. Srinivasan and J.P. Biberian (Eds.), p.257, 6 Feb.–11, 2011.